2022 AIAA SciTech Forum

Higher-Order Approximations for Stabilizing Zero-Energy Modes in Peridynamics Crystal Plasticity Models with Large Horizon Interactions

Iman Javaheri

PhD Candidate, Aerospace Engineering,
University of Michigan, Ann Arbor, MI

Pathways Student, Durability, Damage Tolerance, & Reliability
NASA Langley Research Center, Hampton, VA

Advisors: Veera Sundararaghavan, Andy Newman

January 03, 2022

E-mail: imanajv@umich.edu

Background

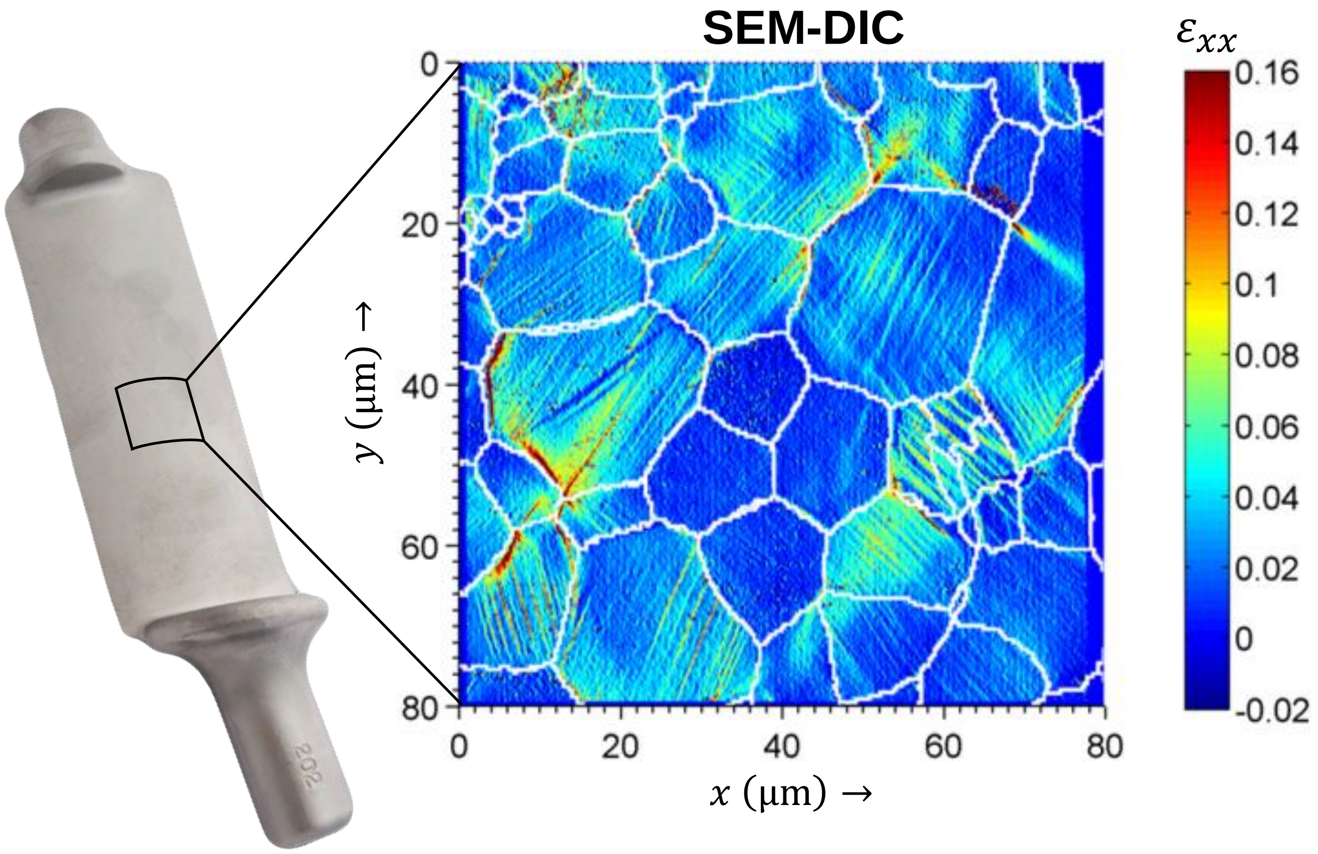

Tensile strain fields of Ti-Al intermetallic turbine blade

Questions

- Can we predict these micro-scale **shear bands** numerically?
- Can any numerical framework **naturally** handle high-strain gradients and cracks?
- Is Peridynamics numerical method accurate, **stable**, and efficient?

State-Based Peridynamics

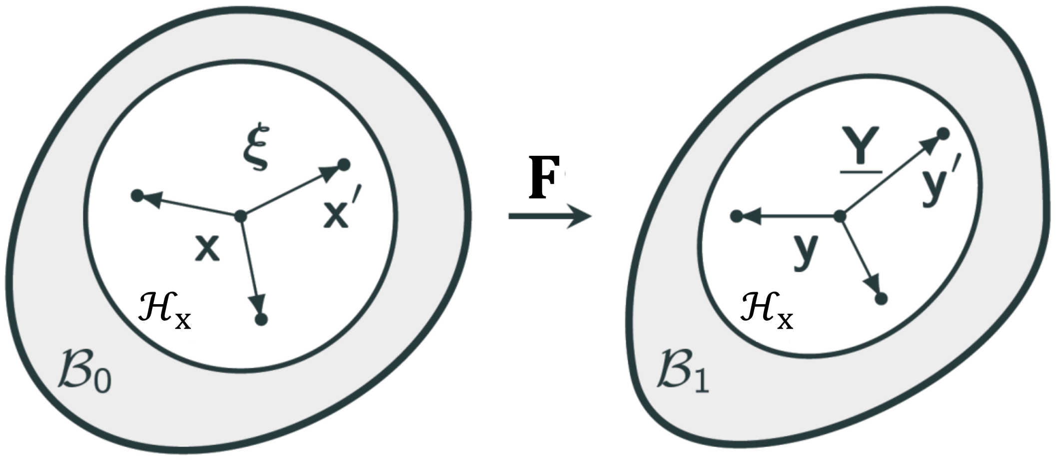

Reference

Current

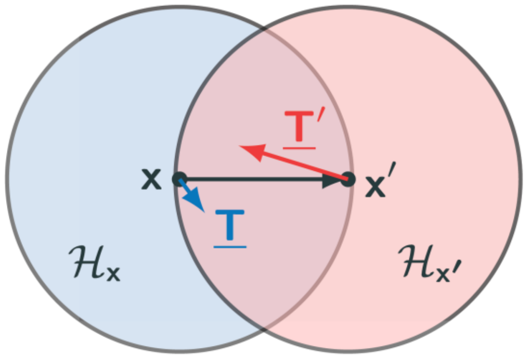

Correspondence Model*

$$\mathbf{F} = \left(\int_{\mathcal{H}_{\mathrm{x}}} \omega \left(\underline{\mathbf{Y}} \otimes \boldsymbol{\xi} \right) dV_{\mathrm{x}'} \right) \mathbf{K}^{-1}$$

bond $\boldsymbol{\xi} = \mathbf{x}' - \mathbf{x}$
deformed bond $\underline{\mathbf{Y}} = \mathbf{y}' - \mathbf{y}$
influence function $\omega = \omega(|\boldsymbol{\xi}|)$
shape tensor $\mathbf{K} = \int_{\mathcal{H}_{\mathrm{x}}} \omega(\boldsymbol{\xi} \otimes \boldsymbol{\xi}) dV_{\mathrm{x}'}$

Governing Equation

$$\int_{\mathcal{H}_{\mathrm{x}}} \left\{ \underline{\mathbf{T}}[\mathbf{x}, t]\langle \mathbf{x}' - \mathbf{x} \rangle - \underline{\mathbf{T}}[\mathbf{x}', t]\langle \mathbf{x} - \mathbf{x}' \rangle \right\} dV_{\mathrm{x}'} + \boldsymbol{b} = \rho \ddot{\mathbf{u}}$$

* S. A. Silling, et al., *Journal of Elasticity*, 82.2 (2007): 151-184.

Adaptive Dynamic Relaxation Solver (ADRS)

Consider

$$\ddot{\mathbf{u}} + c\dot{\mathbf{u}} = \mathbf{f}(\mathbf{u}, \mathbf{x}, t)$$
$$\mathbf{f}(\mathbf{u}, \mathbf{x}, t) = \mathbf{L}/\rho$$

Newmark's scheme (central difference on t):

$$\mathbf{u}^{n+1} = \frac{4\mathbf{u}^n + (c\Delta t - 2)\mathbf{u}^{n-1} + 2\Delta t^2 \mathbf{f}^n}{2 + c\Delta t}$$

Time Step Δt*

$$\Delta t \leq f(h, \delta)\sqrt{\rho/E_{max}}$$

Damping Ratio c**

$$c^n = 2\sqrt{\frac{(\mathbf{u}^n)^T \mathbf{k}^n \mathbf{u}^n}{(\mathbf{u}^n)^T \mathbf{u}^n}}$$
$$\mathrm{k}_{ii}^n = -(\mathrm{f}_i^n - \mathrm{f}_i^{n-1})/(\mathrm{u}_i^n - \mathrm{u}_i^{n-1})$$

Convergence Condition

$e_1 \sim \|\mathbf{L}\|_2$ and $e_2 \sim \|\delta\mathbf{u}\|_2$

* J. Luo, et al., *International Journal of Solids and Structures*, 130 (2017): 36-48.
** B. Kilic, et al., *Theoretical and Applied Fracture Mechanics*, 53.3 (2010): 194-204.

Algorithm Flowchart

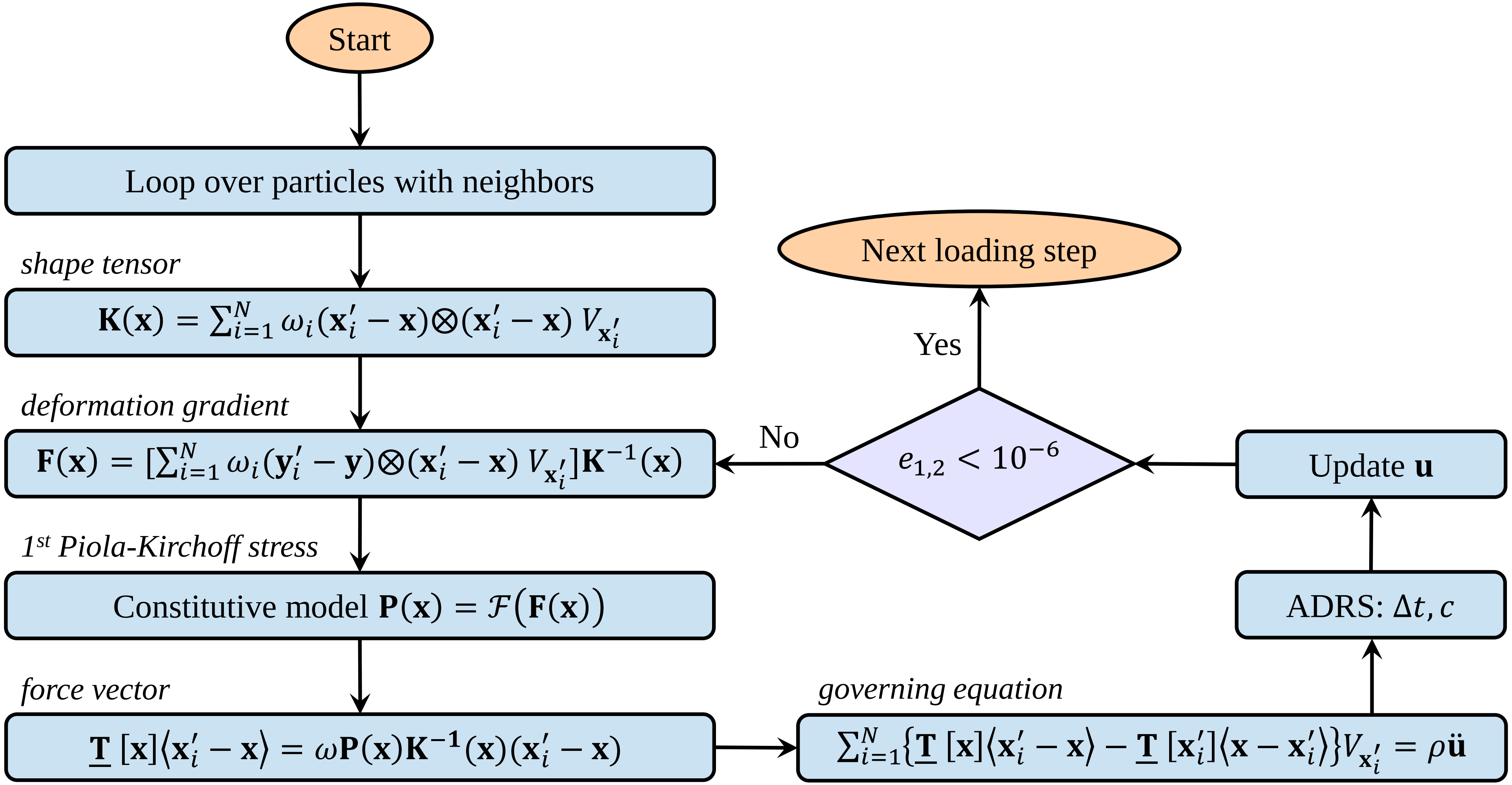

Zero-Energy Modes

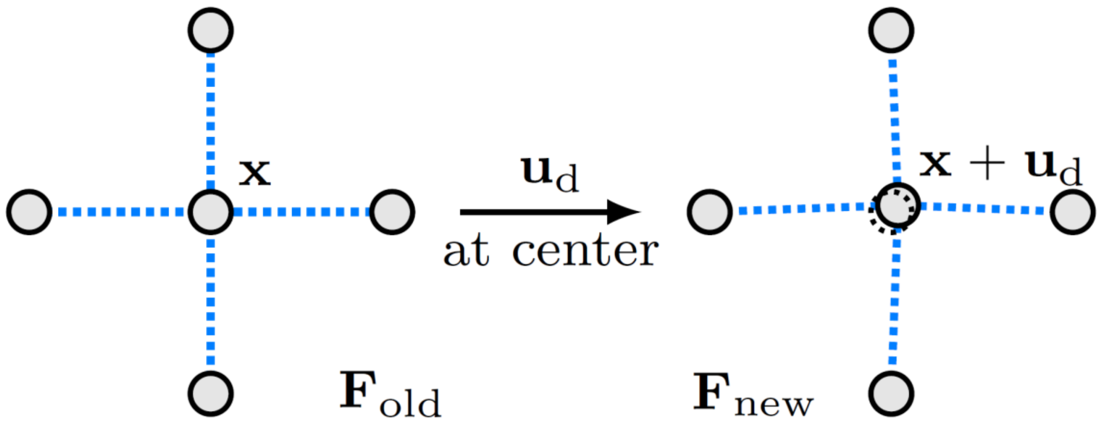

Gradient Tensor

$$\mathbf{F}_{\mathrm{new}} = \left(\int_{\mathcal{H}_{\mathrm{x}}} \omega \left(\underline{\mathbf{Y}}_{\mathrm{new}} \otimes \boldsymbol{\xi} \right) dV_{\mathrm{x}'} \right) \mathbf{K}^{-1}$$

$$= \left(\int_{\mathcal{H}_{\mathrm{x}}} \omega \left[\left(\underline{\mathbf{Y}}_{\mathrm{old}} - \mathbf{u}_{\mathrm{d}} \right) \otimes \boldsymbol{\xi} \right] dV_{\mathrm{x}'} \right) \mathbf{K}^{-1}$$

$$= \mathbf{F}_{\mathrm{old}} - \mathbf{u}_{\mathrm{d}} \otimes \int_{\mathcal{H}_{\mathrm{x}}} \omega \boldsymbol{\xi} dV_{\mathrm{x}'} \, \mathbf{K}^{-1}$$

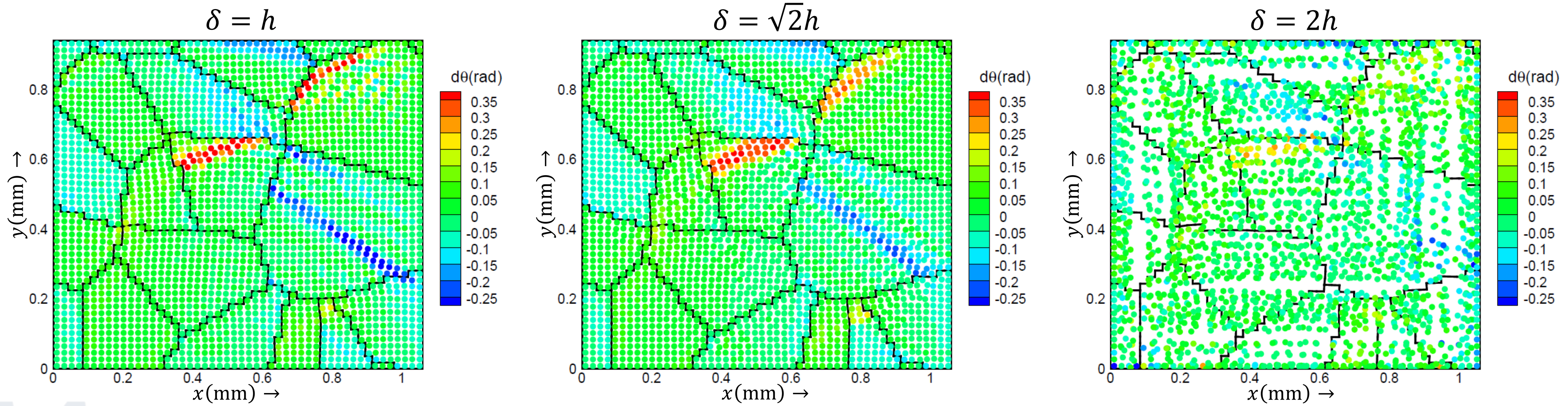

Effect of zero-energy modes on different horizon sizes

Control of Zero-Energy Modes

1. Supplementary Particle Forces

$$\underline{\mathbf{T}}[\mathbf{x}, t]\langle \mathbf{x}' - \mathbf{x} \rangle = \omega \mathbf{P} \mathbf{K}^{-1} \boldsymbol{\xi} + \underline{\mathbf{T}}_{\mathrm{a}}[\mathbf{x}]\langle \mathbf{x}' - \mathbf{x} \rangle$$

2. Stress-Point Approach

$$\mathbf{F} = \frac{1}{2}(\mathbf{F}_{s1} + \mathbf{F}_{s2}) \ \text{ or } \ \boldsymbol{\sigma} = \frac{1}{2}(\boldsymbol{\sigma}_{s1} + \boldsymbol{\sigma}_{s2})$$

3. Higher-Order Approximations

$$\mathbf{F} = \left(\int_{\mathcal{H}_{\mathbf{x}}} \omega (\underline{\mathbf{Y}} \otimes \boldsymbol{\xi}) dV_{\mathbf{x}'} \right) \mathbf{K}^{-1} \approx \partial \mathbf{y} / \partial \mathbf{x}$$

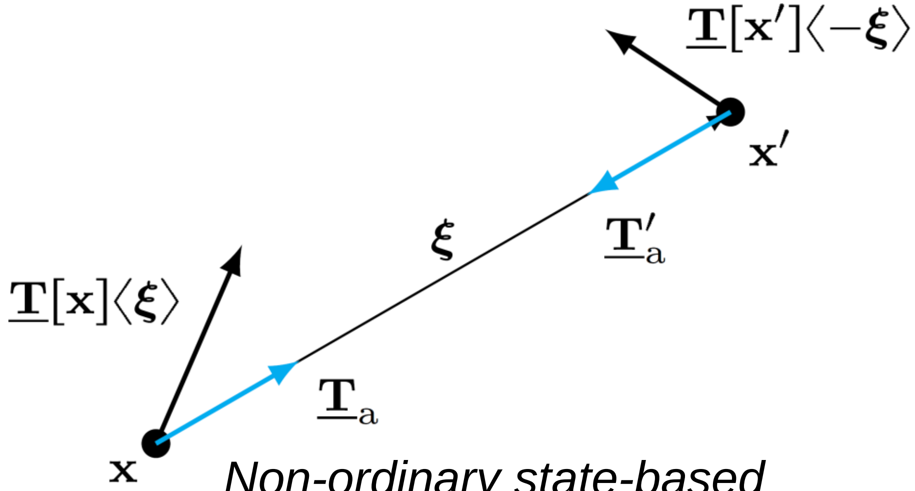

Non-ordinary state-based

- Springs*:

$$\underline{\mathbf{T}}_{\mathrm{a}}[\mathbf{x}] = C_1 \omega [\mathbf{u}(\mathbf{x}') - \mathbf{u}(\mathbf{x})]$$

- Average displacement states**:

$$\underline{\mathbf{T}}_{\mathrm{a}}[\mathbf{x}] = C_2 \int_{\mathcal{H}} \omega [\mathbf{u}(\mathbf{x}') - \mathbf{u}(\mathbf{x})] \, dV_{\mathbf{x}'}$$

* M.S. Breitenfeld, et al., *Computational Methods Applied Mechanical Engineering*, 272, (2014): 233-250.
** S.A. Silling, *Computational Methods Applied Mechanical Engineering*, 322, (2017): 42-57.

Control of Zero-Energy Modes

1. Supplementary Particle Forces

$$\underline{\mathbf{T}}[\mathbf{x}, t]\langle \mathbf{x}' - \mathbf{x} \rangle = \omega \mathbf{P} \mathbf{K}^{-1} \boldsymbol{\xi} + \underline{\mathbf{T}}_{\mathrm{a}}[\mathbf{x}]\langle \mathbf{x}' - \mathbf{x} \rangle$$

2. Stress-Point Approach

$$\mathbf{F} = \frac{1}{2}(\mathbf{F}_{\mathrm{s}1} + \mathbf{F}_{\mathrm{s}2}) \text{ or } \boldsymbol{\sigma} = \frac{1}{2}(\boldsymbol{\sigma}_{\mathrm{s}1} + \boldsymbol{\sigma}_{\mathrm{s}2})$$

3. Higher-Order Approximations

$$\mathbf{F} = \left(\int_{\mathcal{H}_{\mathbf{x}}} \omega (\underline{\mathbf{Y}} \otimes \boldsymbol{\xi}) dV_{\mathbf{x}'} \right) \mathbf{K}^{-1} \approx \partial \mathbf{y} / \partial \mathbf{x}$$

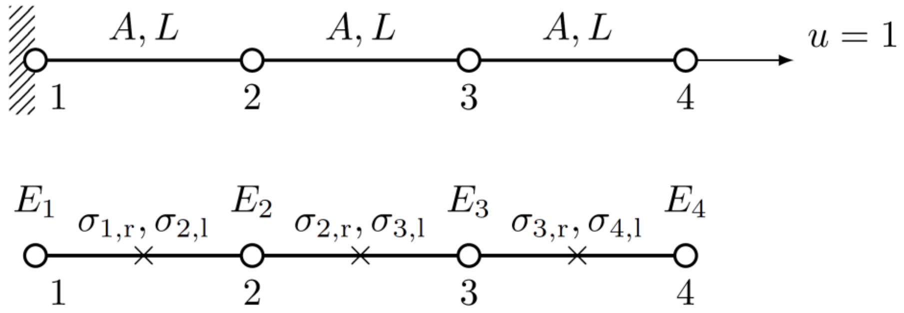

1D Domain

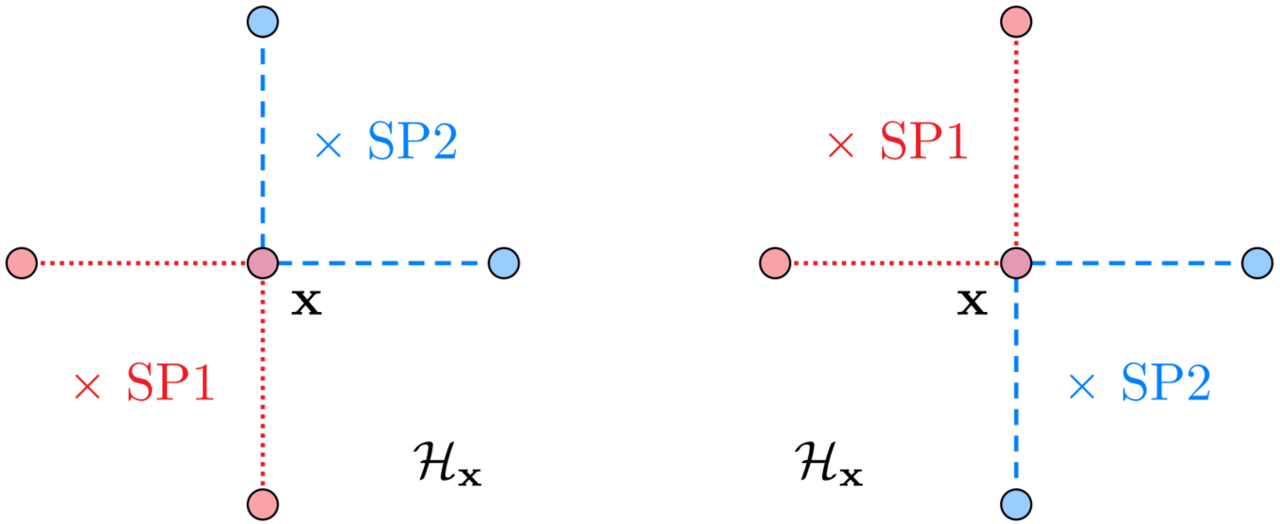

2D Domain

* J. Luo, et al., *International Journal of Solids and Structures*, 150 (2018): 197-207.

Control of Zero-Energy Modes

1. Supplementary Particle Forces

$$\underline{\mathbf{T}}[\mathbf{x},t]\langle\mathbf{x}'-\mathbf{x}\rangle = \omega \mathbf{P}\mathbf{K}^{-1}\boldsymbol{\xi} + \underline{\mathbf{T}}_a[\mathbf{x}]\langle\mathbf{x}'-\mathbf{x}\rangle$$

2. Stress-Point Approach

$$\mathbf{F} = \frac{1}{2}\left(\mathbf{F}_{s1} + \mathbf{F}_{s2}\right) \text{ or } \boldsymbol{\sigma} = \frac{1}{2}\left(\boldsymbol{\sigma}_{s1} + \boldsymbol{\sigma}_{s2}\right)$$

3. Higher-Order Approximations

$$\mathbf{F} = \left(\int_{\mathcal{H}_x} \omega\left(\underline{\mathbf{Y}} \otimes \boldsymbol{\xi}\right) dV_{x'}\right) \mathbf{K}^{-1} \approx \partial \mathbf{y}/\partial \mathbf{x}$$

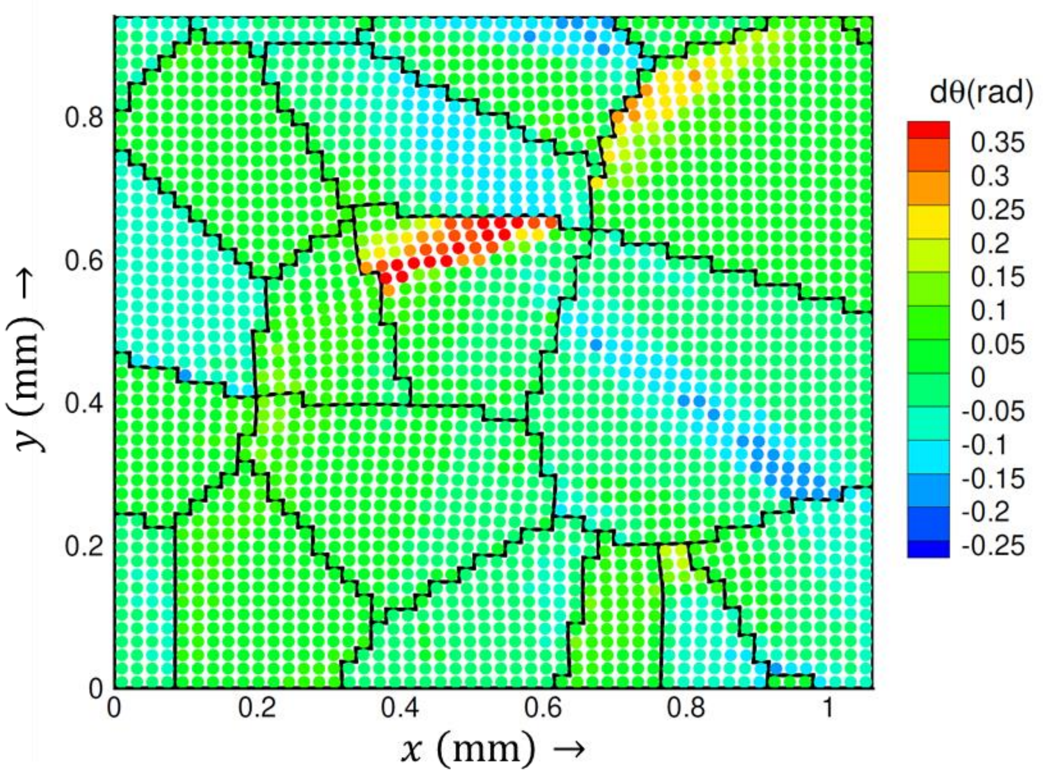

Orientation changes with nearest-neighbor horizon $\delta = h$

* J. Luo, et al., *International Journal of Solids and Structures*, 150 (2018): 197-207.

Control of Zero-Energy Modes

1. Supplementary Particle Forces

$$\underline{\mathbf{T}}[\mathbf{x}, t]\langle \mathbf{x}' - \mathbf{x}\rangle = \omega \mathbf{P}\mathbf{K}^{-1}\boldsymbol{\xi} + \underline{\mathbf{T}}_a[\mathbf{x}]\langle \mathbf{x}' - \mathbf{x}\rangle$$

2. Stress-Point Approach

$$\mathbf{F} = \frac{1}{2}(\mathbf{F}_{s1} + \mathbf{F}_{s2}) \ \text{ or } \ \boldsymbol{\sigma} = \frac{1}{2}(\boldsymbol{\sigma}_{s1} + \boldsymbol{\sigma}_{s2})$$

3. Higher-Order Approximations

$$\mathbf{F} = \left(\int_{\mathcal{H}_{\mathrm{x}}} \omega(\underline{\mathbf{Y}} \otimes \boldsymbol{\xi}) d\mathrm{V}_{\mathrm{x}'}\right)\mathbf{K}^{-1} \approx \partial\mathbf{y}/\partial\mathbf{x}$$

Taylor series expansion of $\mathbf{F}$ (using *Einstein index notation*):

$$F_{pq} = F_{pq} + \frac{1}{2!\,h^2\Omega} G_{pij} \sum_{a=1}^{N} \omega_a \left(\delta x_i \delta x_j \delta x_q\right)_a + \frac{1}{3!\,h^2\Omega} H_{pijk} \sum_{a=1}^{N} \omega_a \left(\delta x_i \delta x_j \delta x_k \delta x_q\right)_a + \mathcal{O}(h^3)$$

Constraint equation: $\Omega(\omega_1, \omega_2, \omega_3, \dots) \neq 0$

AIAA SHAPING THE FUTURE OF AEROSPACE

Control of Zero-Energy Modes

1. Supplementary Particle Forces

$$\underline{\mathbf{T}}[\mathbf{x},t]\langle\mathbf{x}'-\mathbf{x}\rangle = \omega\mathbf{P}\mathbf{K}^{-1}\boldsymbol{\xi} + \underline{\mathbf{T}}_{\mathrm{a}}[\mathbf{x}]\langle\mathbf{x}'-\mathbf{x}\rangle$$

2. Stress-Point Approach

$$\mathbf{F} = \frac{1}{2}\left(\mathbf{F}_{\mathrm{s}1} + \mathbf{F}_{\mathrm{s}2}\right) \text{ or } \boldsymbol{\sigma} = \frac{1}{2}\left(\boldsymbol{\sigma}_{\mathrm{s}1} + \boldsymbol{\sigma}_{\mathrm{s}2}\right)$$

3. Higher-Order Approximations

$$\mathbf{F} = \left(\int_{\mathcal{H}_{\mathbf{x}}} \omega\left(\underline{\mathbf{Y}} \otimes \boldsymbol{\xi}\right) d\mathrm{V}_{\mathbf{x}'}\right)\mathbf{K}^{-1} \approx \partial\mathbf{y}/\partial\mathbf{x}$$

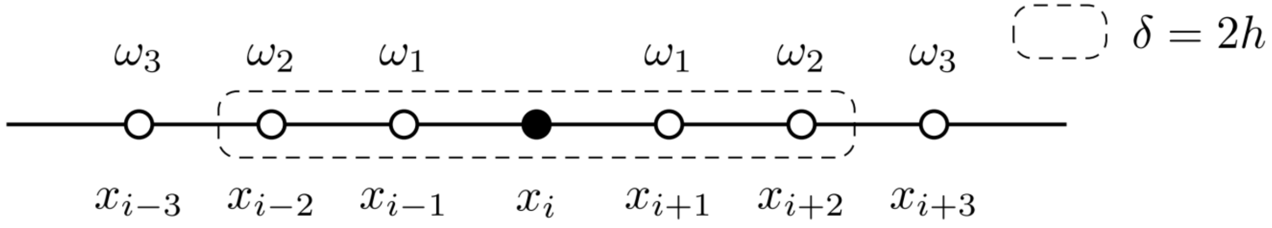

1D particle-discretized bar w/ constant spacing h

discrete weight function values for 1D domain

Horizon Size	Weight Function Values				Leading Error
	ω_1	ω_2	ω_3	ω_4	
$\delta = h$	1	0	0	0	$\mathcal{O}(h^2)$
$\delta = 2h$	1	$-1/16$	0	0	$\mathcal{O}(h^4)$
$\delta = 3h$	1	$-1/10$	$1/135$	0	$\mathcal{O}(h^6)$
$\delta = 4h$	1	$-1/8$	$1/63$	$-1/896$	$\mathcal{O}(h^8)$

1D Numerical Example

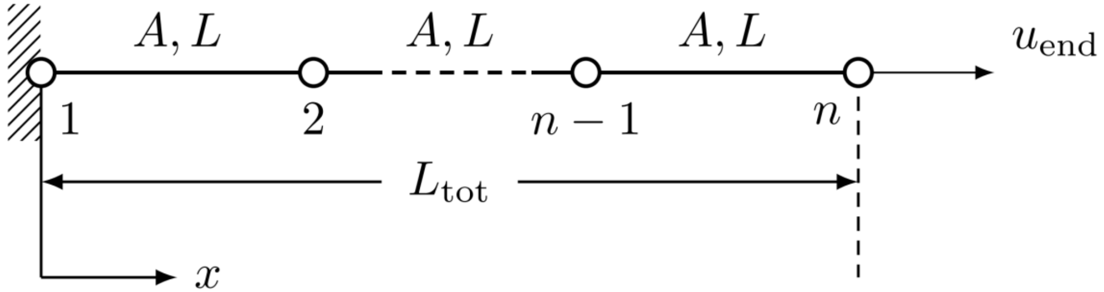

1D discretized cantilever bar

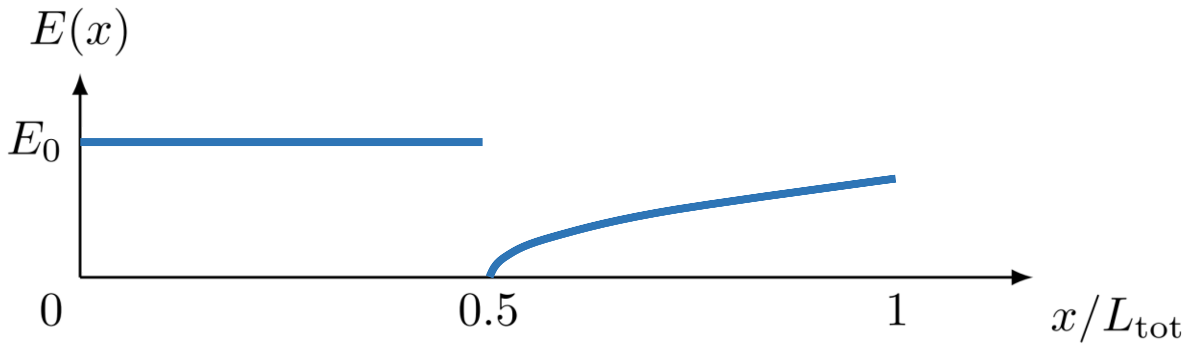

Variable Young's modulus of elasticity

Elastic Cantilever Bar

- Variable elastic modulus
- Analytical displacement $u(x)$:

$$u(x) = \begin{cases} \alpha x & 0 \le x \le \dfrac{L_{tot}}{2} \\ \alpha x + \beta L_{tot}\sqrt{\dfrac{x}{L_{tot}} - \dfrac{1}{2}} & \dfrac{L_{tot}}{2} < x \le L_{tot} \end{cases}$$

where $\alpha = 0.001, \beta = 0.004\sqrt{2}, L_{tot} = 1$

Mesh Size

500 equally-distant particles

Boundary Condition

$u_{end} = 0.005 L_{tot}$

1D Numerical Example

Horizon size: $2h$

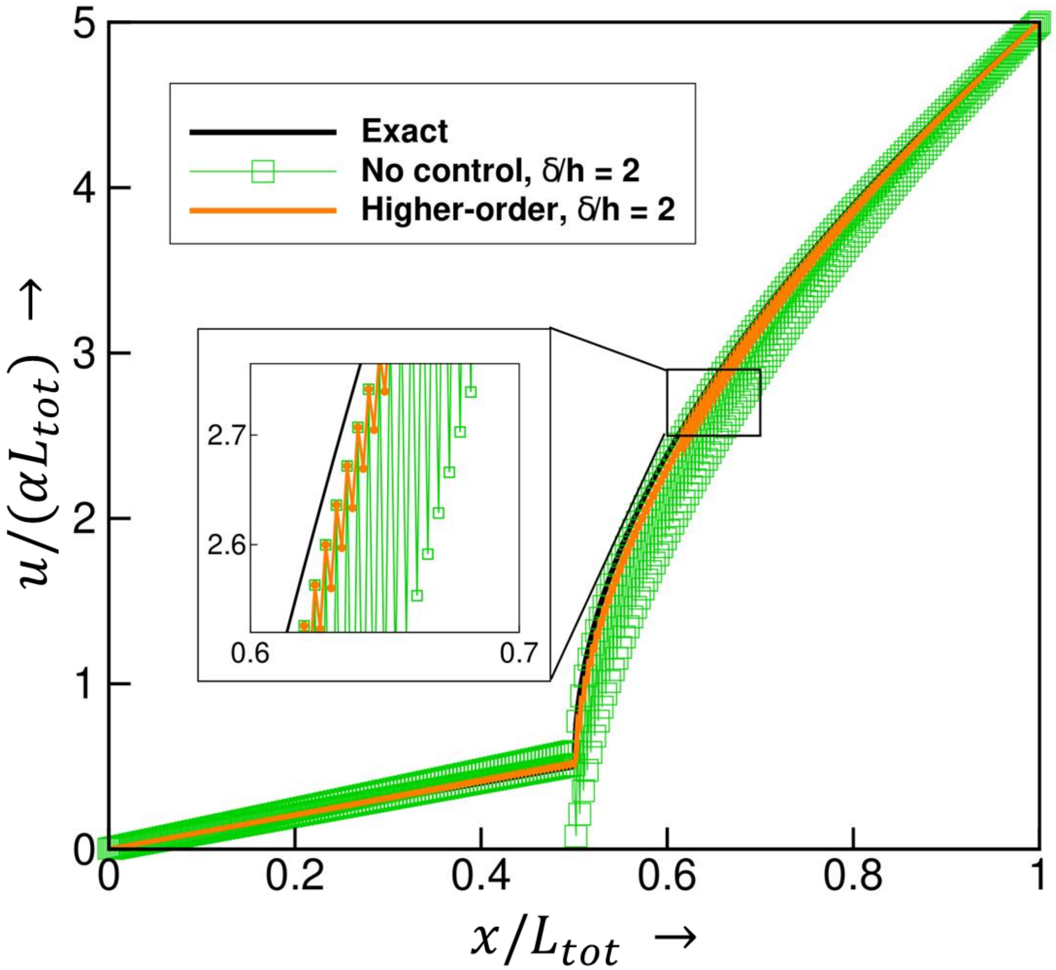

Elastic Cantilever Bar

- Variable elastic modulus
- Analytical displacement $u(x)$:

$$u(x) = \begin{cases} \alpha x & 0 \leq x \leq \frac{L_{tot}}{2} \\ \alpha x + \beta L_{tot}\sqrt{\frac{x}{L_{tot}} - \frac{1}{2}} & \frac{L_{tot}}{2} < x \leq L_{tot} \end{cases}$$

where $\alpha = 0.001, \beta = 0.004\sqrt{2}, L_{tot} = 1$

Mesh Size

500 equally-distant particles

Boundary Condition

$u_{end} = 0.005L_{tot}$

1D Numerical Example

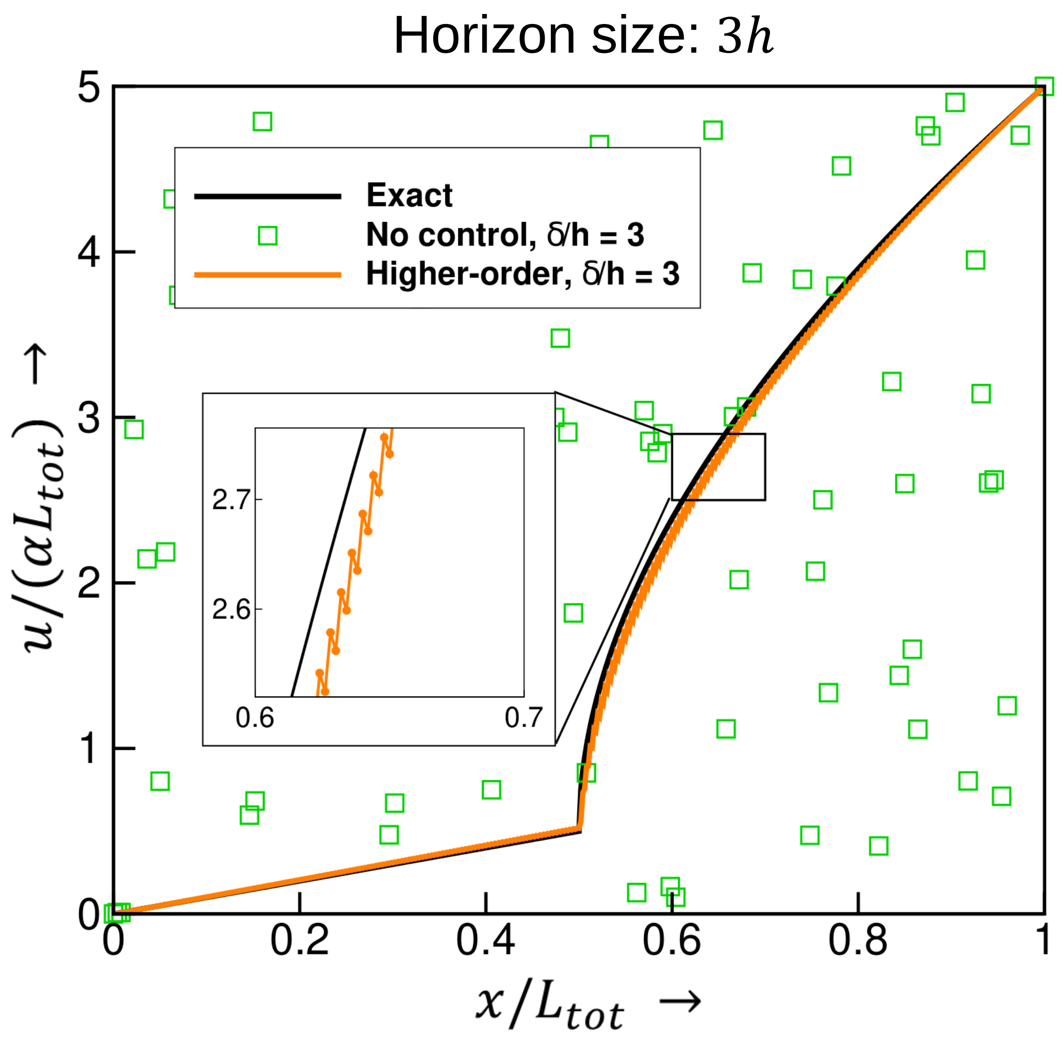

Elastic Cantilever Bar

- Variable elastic modulus
- Analytical displacement $u(x)$:

$$u(x) = \begin{cases} \alpha x & 0 \le x \le \dfrac{L_{tot}}{2} \\ \alpha x + \beta L_{tot}\sqrt{\dfrac{x}{L_{tot}} - \dfrac{1}{2}} & \dfrac{L_{tot}}{2} < x \le L_{tot} \end{cases}$$

where $\alpha = 0.001, \beta = 0.004\sqrt{2}, L_{tot} = 1$

Mesh Size

500 equally-distant particles

Boundary Condition

$u_{end} = 0.005 L_{tot}$

2D Numerical Example

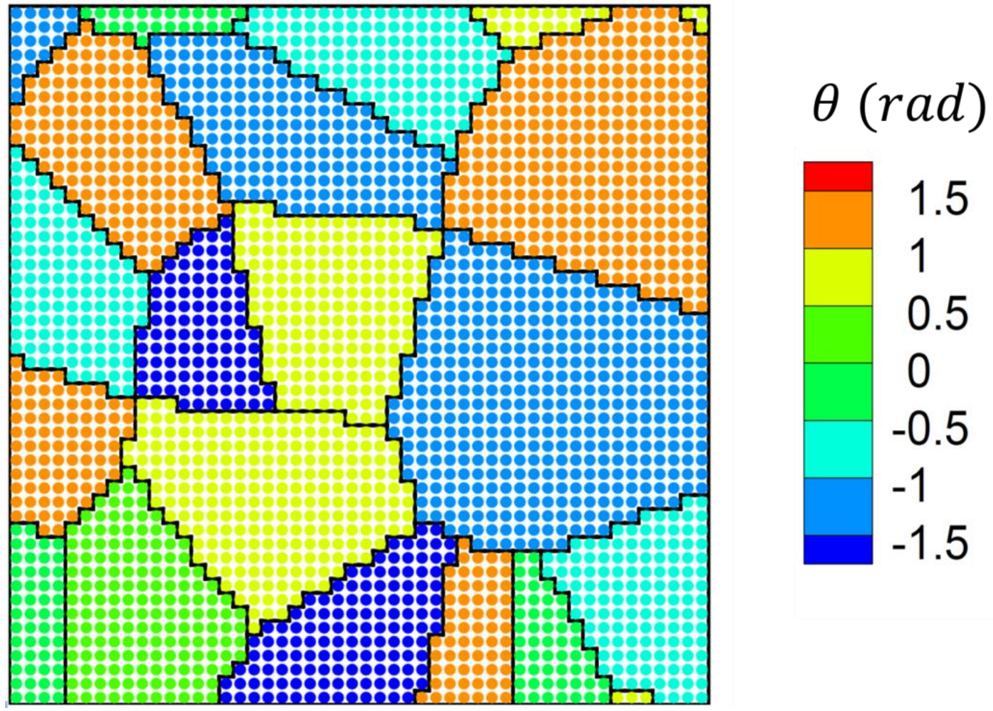

Orientation distributions

Polycrystals

- 21 grains (*Voronoi tessellation*)
- 2 slip systems with hardening rule*:

$$h^{\alpha\beta} = h_0^{\beta}\left(q + (1-q)\delta^{\alpha\beta}\right)\left(1 - \frac{s^{\beta}(t)}{s_s^{\beta}}\right)^{a}$$

Mesh Size

- Uniform 50×50 particles

Boundary Condition

- Velocity gradient
- Performed in 30 steps

* S. Sun, et al., *International Journal of Solids and Structures*, 51.19 (2014): 3350-3360.

2D Numerical Example

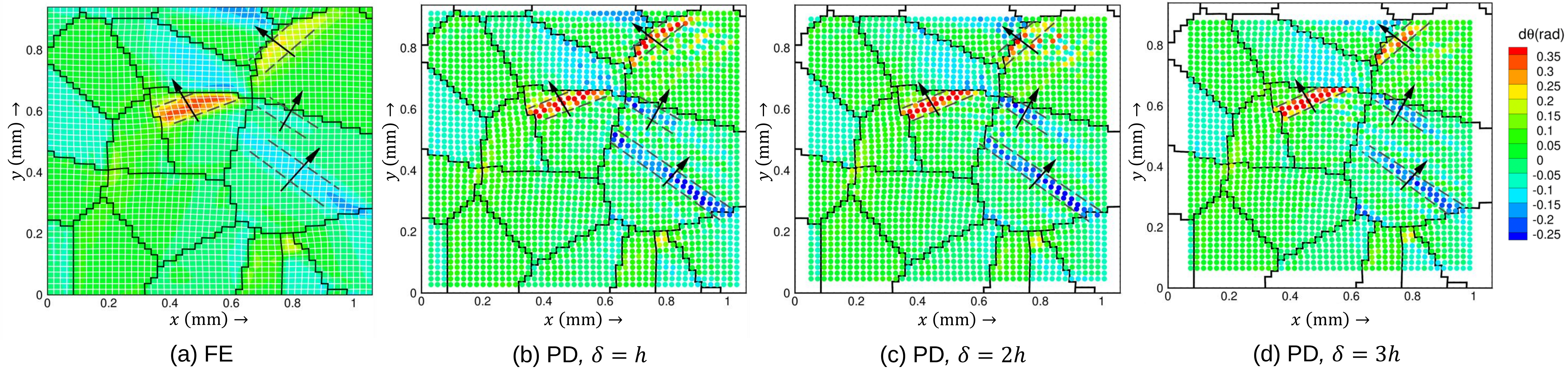

Orientation changes for 2500 particles under a y-axis compression test obtained from crystal plasticity finite element (FE) and peridynamics (PD) simulations with different horizon sizes δ

3D Matrix with Soft Precipitate

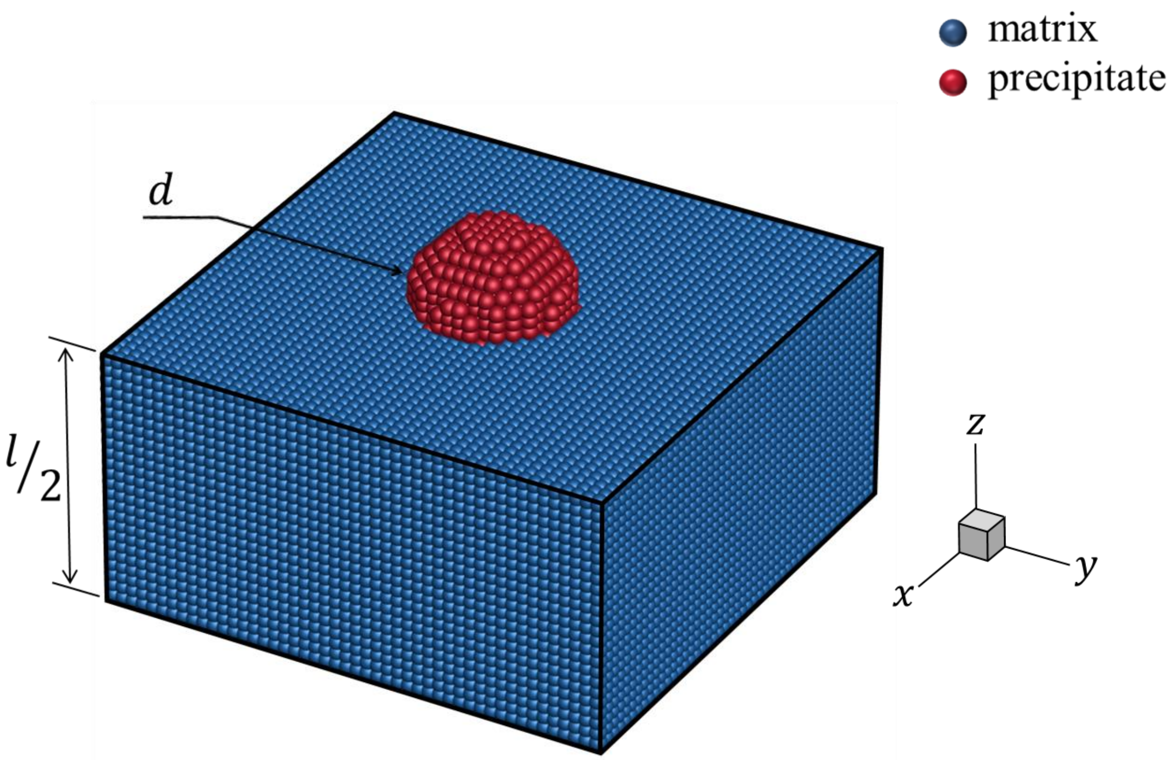

Composite

- Transversely-isotropic elastic matrix with dimension $l = 3.0\ \mathrm{mm}$
- Soft precipitate with stiffness ratios $r_c = 1, 10^{-1}, \ldots, 10^{-5}$ and diameter $d = 0.875\ \mathrm{mm}$ at the center

$$\boldsymbol{C}^{ppt} = r_c\, \boldsymbol{C}^{\mathbf{mat}}$$

Mesh Size

- Uniform $48 \times 48 \times 48$ grid

Boundary Condition

- Velocity gradient:

$$\mathbf{L} = \mathrm{diag}(1.0, -0.5, -0.5)$$

3D Matrix with Soft Precipitate

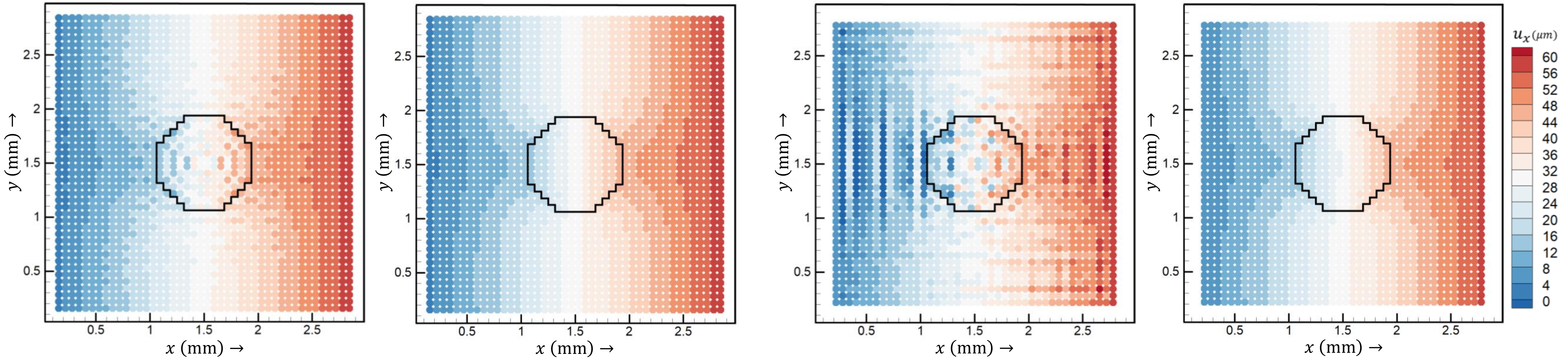

(a) No control, $\delta = 2h$ (b) Higher-order, $\delta = 2h$ (c) No control, $\delta = 3h$ (d) Higher-order, $\delta = 3h$

*Displacements under x-axis tension obtained from peridynamics models with "**No Control**" of zero-energy modes against proposed "**Higher-Order**" stabilization approach for $\delta = 2h$ and $3h$ at midsection $z = 1.5\ mm$*

3D Matrix with Soft Precipitate

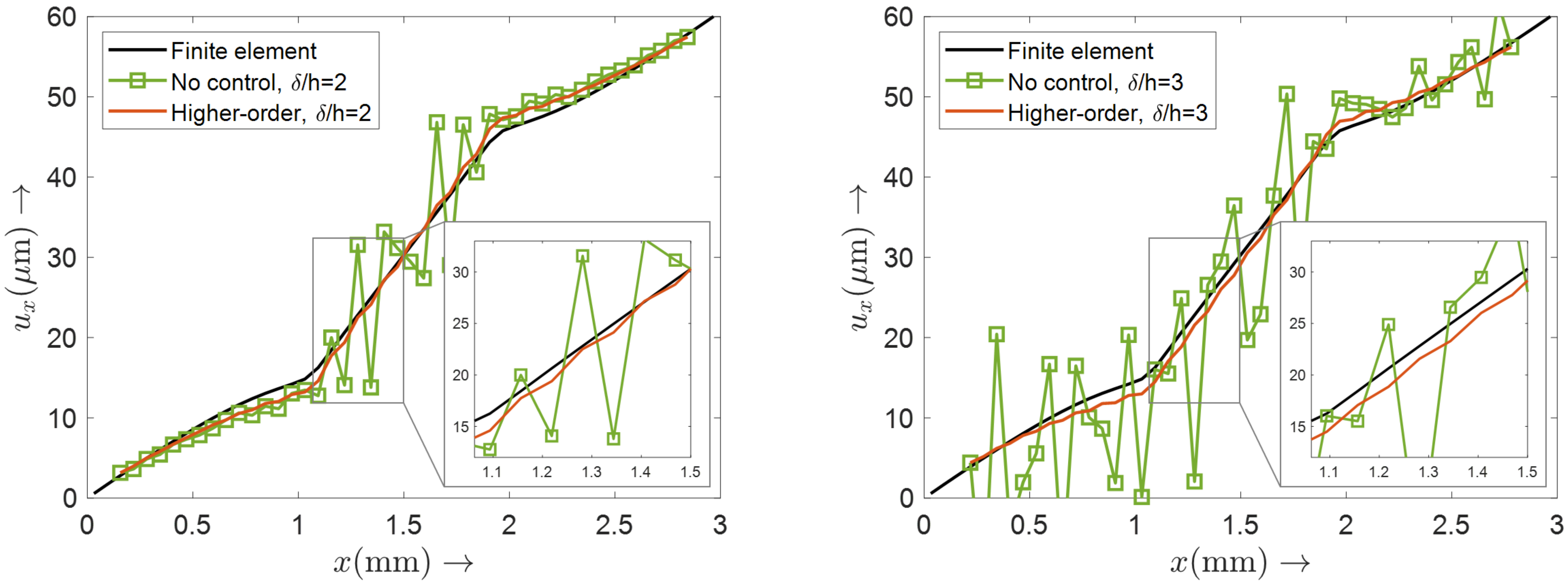

(a) $\delta = 2h$ (b) $\delta = 3h$

Displacements through centerline for two horizon interactions along midsection $z = 1.5\ mm$

3D Matrix with Soft Precipitate

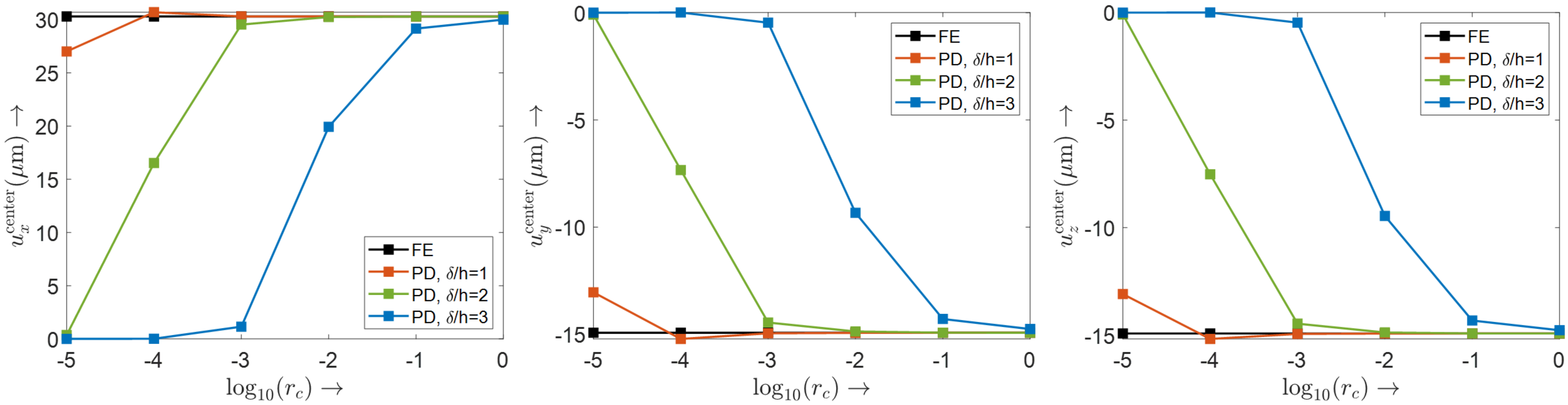

Variations in the displacement components at the center of the spherical precipitate in terms of the stiffness ratio r_c for different horizon sizes δ

3D Polycrystalline with Void

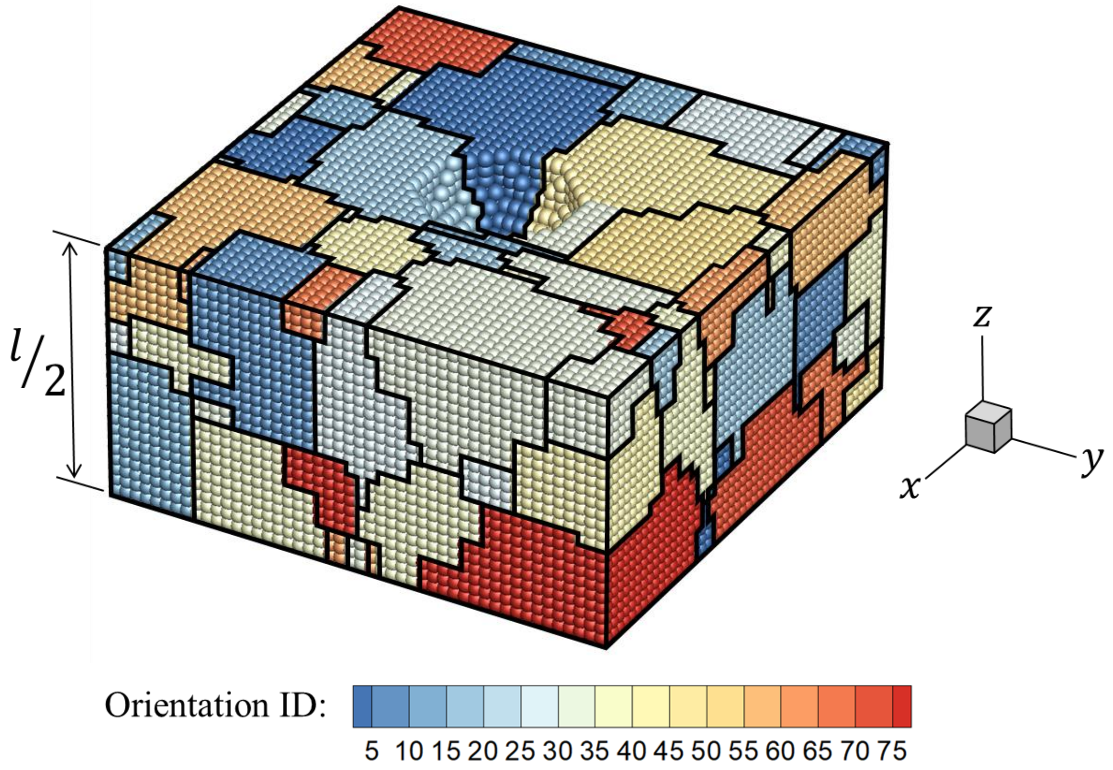

Polycrystals

- WE43 alloy-T5 temper w/ 78 grains
- 18 slip systems*
- Soft precipitate w/ stiffness ratio $r_c = 0.1$ and $d = 0.875\ \mathrm{mm}$ at the center

Mesh Size

- Uniform $48 \times 48 \times 48$ grid

Boundary Condition

- Velocity gradient:

$$\mathbf{L} = \mathrm{diag}(1.0, -0.5, -0.5)$$

* A. Lakshmanan, et al., *International Journal of Plasticity*, 142 (2021): 102991.

3D Polycrystalline with Void

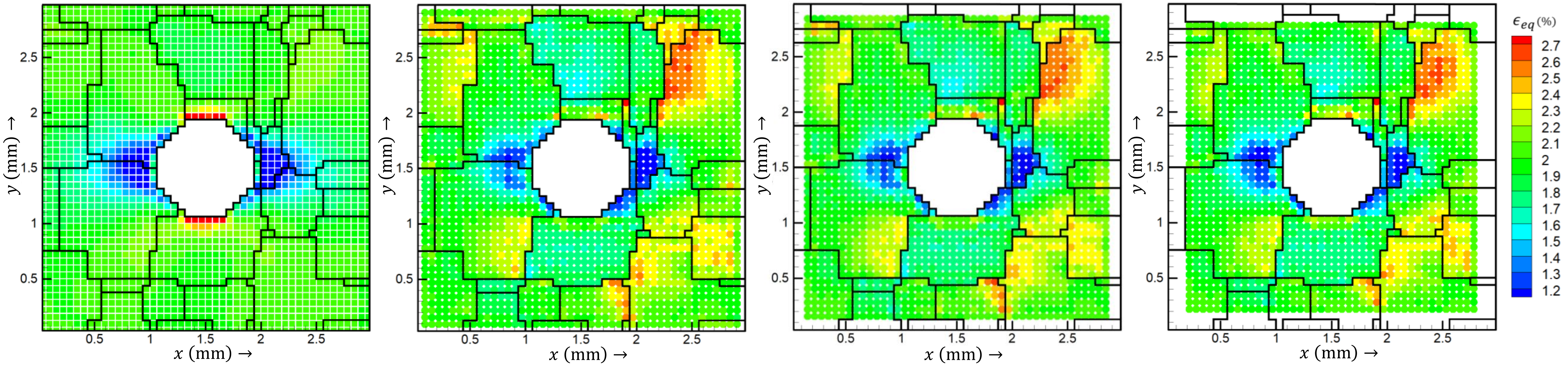

(a) FE (b) PD, $\delta = h$ (c) PD, $\delta = 2h$ (d) PD, $\delta = 3h$

Equivalent strains under x-axis tension test obtained from crystal plasticity finite element (FE) and peridynamics (PD) simulations with different horizon sizes δ at midsection $z = 1.5\ mm$

Summary

1. Background
2. State-Based Peridynamics with Adaptive Dynamic Relaxation Solver (PD-ADRS)
3. Control of Zero-Energy Modes
4. Higher-Order Approximation Weight Functions
5. Multi-Dimensional Numerical Examples
6. Summary

UNIVERSITY OF MICHIGAN

Thank You

Questions can be directed to imanajv@umich.edu.

AIAA
SHAPING THE FUTURE OF AEROSPACE